Research on the compact TE$_{01}$-TE$_{11}$ elliptical waveguide mode converter in Ka-band

ZHAO Lian-Min， LIU Jian-Wei[*]， WANG Li-Na， QING Jie， JIA Kai， SUN Zong-Zheng

（School of Electronic Science and Engineering，University of Electronic Science and Technology of China，
Chengdu 610054，China）

Abstract：In this article, the elliptic waveguide TE$_{01}$-TE$_{11}$ mode converter is studied. The proper elliptical waveguide cross section is selected, the phase re-matching method is used in the elliptical waveguide longitudinal contour line function, and the longitudinal contour line optimization is performed using a particle swarm algorithm, and the designed elliptical TE$_{01}$-TEs$_{11}$ mode converter has a conversion efficiency of 99. 16% at 28 GHz. The efficiency of the mode converter at 27-29. 3 GHz is more than 90%, and the relative bandwidth is 8. 2%. The conversion section of the designed TE$_{01}$-TEs$_{11}$ elliptic mode converter is half of the existing length. The designed elliptical mode converter is connected to two transition segments and simulated and verified in CST, and the results are consistent with the theoretical calculations. An efficient, compact, high-power elliptical waveguide TE$_{01}$-TE$_{11}$ mode converter with a center frequency point of 28 GHz is designed.

Key words：elliptical waveguide, mode converter, high efficiency, broadband

Ka 波段紧凑型 TE$_{01}$-TE$_{11}$ 椭圆波导模式转换器的研究

赵连敏， 刘建卫[*]， 王丽娜， 卿 捷， 贾 凯， 孙宗正
（电子科技大学 电子科学与工程学院，四川 成都 610054）

摘要：本文对椭圆波导 TE$_{01}$-TE$_{11}$ 模式转换器进行了研究。选择了合适的椭圆波导截面，在椭圆波导纵轮廓线函数中采用了相位重匹配方法，并利用粒子群算法进行了纵轮廓线优化，所设计的椭圆 TE$_{01}$-TEs$_{11}$ 模式转换器在 28 GHz 时的转换效率为 99.16%，在 27~29.3 GHz 模式变换器的效率大于 90%，相对带宽为 8.2%。所设计的 TE$_{01}$-TEs$_{11}$ 椭圆模式转换器的转换段为现有长度的一半。将设计的椭圆模式转换器与两个过渡段相连，并在 CST 中进行仿真和验证，其结果与理论计算一致。设计出了一个中心频率点为 28 GHz 的高效、紧凑、高功率椭圆波导 TE$_{01}$-TE$_{11}$ 模式转换器。

关 键 词：椭圆波导；模式转换器；高效率；宽带

中图分类号：TN129   **文献标识码**：A

Introduction

Elliptical waveguides are a type of waveguides that have a wide range of applications in satellite communications, antenna feed systems for radar, and research on accelerating tube[1]. Elliptical waveguides are generally flexible and bendable, with more stable waveform transmission. And it is easy to be manufactured in large lengths, up to several hundred meters.

As an important high-power microwave source, the cyclotron has a wide range of applications in high-performance radar, phased-array radar, millimeter-wave communications, controlled thermonuclear fusion and other systems[2-4]. High-power microwave transmission generally uses circular waveguide mode converters or quasi-optical mode converters, and in some practical applications, traditional mode converters sometimes cannot meet the project requirements. Based on the coupling wave theory and phase re-matching technique, the conventional circu-

lar waveguide TE$_{01}$-TE$_{11}$ mode converter for transmitting high power microwave can be designed and analyzed by numerical calculation and simulation. With the improvement of the periodic structure, the efficiency of the conventional mode converter is also improved. However, the bandwidth of the conventional circular waveguide TE$_{01}$-TE$_{11}$ mode converter cannot be satisfied the requirements of microwave transmission [5-7].

While circular waveguide mode converters are relatively fixed in cross-section and cannot be fine-tuned in cross-section, elliptical waveguides are better able to increase or suppress the coupling ability between certain modes according to the design requirements and thus improve efficiency due to their deformable cross-section. At the same time, elliptical waveguide devices have a larger bandwidth than circular waveguide devices. Therefore, it is necessary to study elliptical waveguide mode converters. Although the existing TE$_{01}$-TE$_{11}$ elliptical waveguide mode converter achieves wide bandwidth, it is twice as long as the circular waveguide mode converter and is not compact enough [8-9].

In this paper, an elliptic waveguide TE$_{01}$-TE$_{11}$ mode converter operating at 28 GHz at the center frequency is designed. This mode converter consists of a section of elliptic waveguide TE$_{01}$-TEs$_{11}$ mode converter and its two input and output transitions.

1 Working principle

When the elliptical waveguide contour line is changed, the coupling between the modes in the waveguide is also changed. Coupled wave equations in elliptic waveguides [10-12].

$$\begin{cases} \dfrac{dA^{+}_{m'n'}}{dw} = -j\beta_{m'n'}A^{+}_{m'n'} - j\sum_{mn}\left[C^{+}_{(mn')(mn)}A^{+}_{mn} + C^{-}_{(mn')(mn)}A^{-}_{mn} \right] \\ \dfrac{dA^{-}_{m'n'}}{dw} = j\beta_{m'n'}A^{-}_{m'n'} + j\sum_{mn}\left[C^{-}_{(mn')(mn)}A^{+}_{mn} + C^{+}_{(m'n')(mn)}A^{-}_{mn} \right] \end{cases} \tag{1}$$

where A^{+}_{mn} and A^{-}_{mn} represent the forward and reverse waves, respectively. $C^{+}_{(m'n')(mn)}$ and $C^{-}_{(m'n')(mn)}$ denote the coupling coefficients and directions between the modes $m'n'$ and mn. $\gamma_{m'n'}$ is the propagation constant, $\gamma_{m'n'} = \alpha_{m'n'} + j\beta_{m'n'}$, where $\alpha_{m'n'}$ is the decay constant, $\beta_{m'n'}$ is the phase constant, and j is an imaginary number.

For the convenience of expressing the coupling wave coefficients, define:

$$\begin{cases} H_{ii} = \iint_{\Omega} \zeta T^{(i)}_{mn} T^{(i)}_{m'n'} ds \\ H_{\partial ii} = \iint_{\Omega} \zeta \left(\dfrac{\partial T^{(i)}_{mn}}{h_1 \partial \xi} \dfrac{\partial T^{(i)}_{m'n'}}{h_1 \partial \xi} + \dfrac{\partial T^{(i)}_{mn}}{h_2 \partial \eta} \dfrac{\partial T^{(i)}_{m'n'}}{h_2 \partial \eta} \right) ds \\ H_{\partial ij} = \iint_{\Omega} \zeta \left(\dfrac{\partial T^{(i)}_{mn}}{h_1 \partial \xi} \dfrac{\partial T^{(j)}_{m'n'}}{h_2 \partial \eta} - \dfrac{\partial T^{(i)}_{mn}}{h_2 \partial \eta} \dfrac{\partial T^{(j)}_{m'n'}}{h_1 \partial \xi} \right) ds \end{cases} \tag{2}$$

where, $i \neq j$, h$_1$ and h$_2$ are Lamo coefficients. T_{mn} is the solution of Mathieu function.

When bending along the long axis:
$$\zeta = h \sinh \xi \sin \eta \tag{3}$$

when bending along the short axis:
$$\zeta = h \cosh \xi \cos \eta \tag{4}$$

the coupling coefficients of TM-TM mode and TE-TE mode can be expressed as:

$$C^{\pm}_{(m'n')(mn)} = -\frac{j\omega}{2R}\left[T_i \left(\frac{k^{(i)}_{cmn} k^{(i)}_{cm'n'}}{k} \right)^2 H_{ii} + \left(\frac{\pm\mu}{\sqrt{Z^{(i)}_{mn} Z^{(i)}_{m'n'}}} + \varepsilon \sqrt{Z^{(i)}_{mn} Z^{(i)}_{m'n'}} \right) H_{\partial ii} \right] \tag{5}$$

where:

$$T_i = \begin{cases} \mu \dfrac{+1}{\sqrt{Z^{(1)}_{mn} Z^{(1)}_{m'n'}}} & i = 1 \\ -\varepsilon \sqrt{Z^{(2)}_{mn} Z^{(2)}_{m'n'}} & i = 2 \end{cases} \tag{6}$$

the coupling coefficient between TE-TM modes can be expressed as:

$$C^{\pm}_{(m'n')(mn)} = -\frac{j\omega}{2R}\left(\frac{\pm\mu}{\sqrt{Z^{(i)}_{mn} Z^{(j)}_{m'n'}}} + \varepsilon \sqrt{Z^{(i)}_{mn} Z^{(j)}_{m'n'}} \right) H_{\partial ij}. \tag{7}$$

The elliptical waveguide coupling coefficient cannot be expressed by the formula, but can only be obtained by numerical method, and solving for the coupling coefficients requires solving for the Mathieu function [13-14].

The circular waveguide can be regarded as a special elliptic waveguide with $e = 0$. When the eccentricity $e \neq 0$, the elliptic waveguide cross section becomes asymmetric and the TE$_{mn}$ mode divides into TE$_{smn}$ and TE$_{cmn}$ modes, and the TM$_{mn}$ mode divides into TM$_{smn}$ and TM$_{cmn}$ modes, where TE$_{smn}$ and TM$_{smn}$ denote odd modes and TE$_{cmn}$ and TM$_{cmn}$ denote even modes.

When the elliptic symmetry plane is perpendicular to the long axis, the coupling coefficients of TE-TE and TM-TM modes are non-zero only when one is an even mode and the other is an odd mode; the mode coupling coefficients of TE-TM are non-zero only when both modes are either even or odd modes.

When the elliptic symmetry plane is perpendicular to the short axis, the mode coupling coefficients of TE-TE and TM-TM are non-zero only when both modes are even or odd modes; the coupling coefficient of TE-TM mode is non-zero only when one is an even mode and the other is an odd mode.

The expression of the coupling coefficient between modes can be rewritten as:

$$C^{\pm}_{(mn)(m'n')} = \frac{1}{R(w)} \times D^{\pm}_{(mn)(m'n')} \tag{8}$$

for TM-TM mode and TE-TE mode:

$$D^{\pm}_{(m'n')(mn)} = -\frac{j\omega}{2}\left[T_i \left(\frac{k^{(i)}_{cmn} k^{(i)}_{cm'n'}}{k} \right)^2 H_{ii} + \left(\frac{\pm\mu}{\sqrt{Z^{(i)}_{mn} Z^{(i)}_{m'n'}}} + \varepsilon \sqrt{Z^{(i)}_{mn} Z^{(i)}_{m'n'}} \right) H_{\partial ii} \right] \tag{9}$$

for TE-TM mode：

$$D_{(m'n')(mn)}^{\pm} = -\frac{j\omega}{2}\left(\frac{\pm\mu}{\sqrt{Z_{mn}^{(i)}Z_{m'n'}^{(j)}}} + \varepsilon\sqrt{Z_{mn}^{(i)}Z_{m'n'}^{(j)}}\right)H_{\partial ij} . \quad (10)$$

Eq.（8）is composed of transverse and longitudinal components, in which $R(w)$ is the radius of curvature of the longitudinal contour line bend and $D_{(m'n')(mn)}^{\pm}$ is the relative coupling coefficient, which depends only on the cross section of the elliptical waveguide.

Therefore, the design of an efficient, compact, broadband high power elliptic waveguide mode converter requires both the selection of the appropriate cross-sectional dimensions and the proper optimization of its longitudinal direction（disturbance direction of elliptical waveguide）. Next, the proper cross-sectional dimensions are selected first.

2   Numerical calculations and simulation

The central frequency point of the elliptical waveguide mode converter designed in this paper is 28 GHz, the long semi-axis is a=16 mm, the long axis is fixed, and the short axis depends on the selection of the eccentricity. Designing an efficient TE_{01}-TE_{11} elliptic waveguide mode converter requires both improving the TE_{01}-TE_{11} coupling ability and suppressing spurious mode output.

In the elliptical TE_{01}-TE_{11} mode converter, the normalized cutoff wavelengths of the main modes are shown in Fig. 1. In the circular waveguide TE_{01}-TE_{11} mode converter, TE_{01} and TE_{11} belong to the main coupling mode, while in the elliptic waveguide mode changer, the TE_{11} mode is divided into TEs_{11} odd mode and TEc_{11} even mode. As can be seen from the figure, with the increase of elliptic centroid, the difference of normalized cutoff wavelength between TE_{01} and TEs_{11} modes is smaller than the difference of normalized cutoff wavelength between TE_{01} and TEc_{11} modes, which means that the coupling ability between TE_{01} and TEs_{11} is larger than the coupling ability between TE_{01} and TEc_{11}. And the size of the coupling ability determines the mode conversion efficiency of
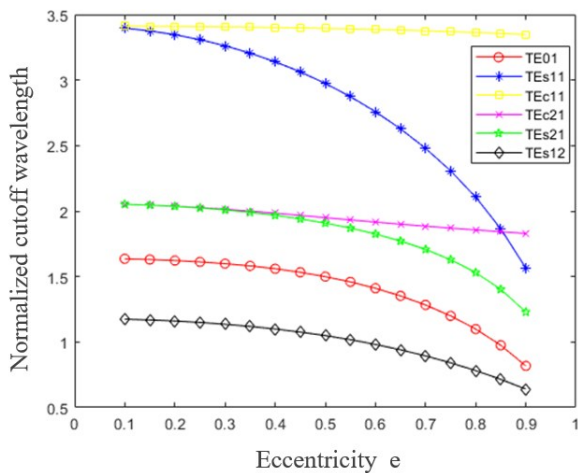

Fig. 1   The major mode normalized cutoff wavelengths in elliptical waveguides
图1   椭圆波导中的主模归一化截止波长

the mode converter, so the coupling between TE_{01} and TEs_{11} is chosen in this paper, i. e., bending toward the direction of the symmetry plane of the elliptical waveguide perpendicular to the long axis.

After determining the bending direction and the main coupling mode of the elliptical waveguide, it is necessary to analyze the stronger spurious modes present in the converter. TEs_{11} will have stronger coupling with TEc_{21}, thus increasing the spurious mode TEc_{21} and thus reducing the output power of TEs_{11} mode; TE_{01} will have stronger coupling with TEs_{12} mode, which will reduce the input power of the input mode TE_{01} and increase the spurious mode TEs_{12}, which affects the conversion of TE_{01} to TEs_{11}. In addition, there are also TEs_{21}, $TMc_{11,}$ TMs_{21} and other heterodyne modes.

Fig. 2 shows the variation pattern of the eccentricity by the coupling coefficients of TE_{01}-TEs_{11} and TEs_{11}-TEc_{21}. Selecting the appropriate eccentricity in the design of TE_{01}-TE_{11} mode converter requires increasing the coupling coefficient of TE_{01}-TEs_{11} and decreasing the coupling coefficient of TEs_{11}-TEc_{21} as much as possible. Therefore, the initial selection of e is 0.65-0.85.
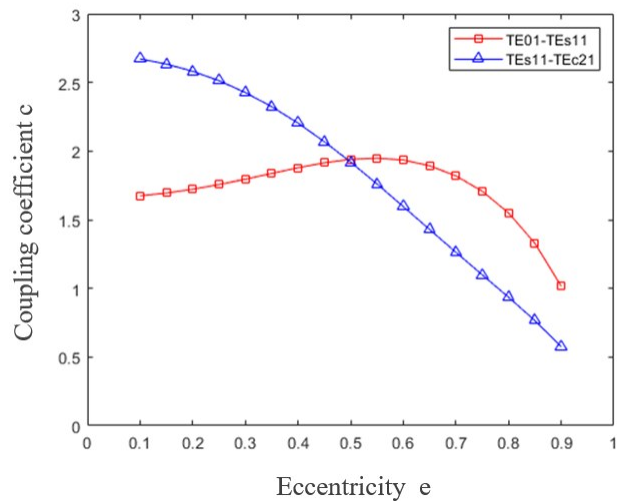

Fig. 2   The variation law of coupling coefficient with eccentricity
图2   耦合系数随离心率的变化规律

Obviously, the coupling ability of the interaction modes depends on the coupling coefficient and the difference of eigenvalues is defined by the following expression: $Q = c/(\beta_m - \beta_n)$, where c is the coupling coefficient between the modes m and n. β_m and β_n are the mode phase constants, respectively. As shown in Fig. 3, the coupling ability between TE_{01}-TEs_{11} remains almost constant between e=0.1-0.5 and gradually decreases to zero after e=0.5. The coupling ability between TEs_{11}-TEc_{21} gradually decreases and shows a sudden change around e=0.85, so the eccentricity is chosen to avoid the vicinity of 0.85. Between 0.1 and 0.9, the coupling ability of TEs_{11}-TEc_{21} is always larger than that of TE_{01}-TEs_{11} regardless of the value of e, that is, the conversion ability of TEs_{11}-TEc_{21} is larger, which brings diffi-
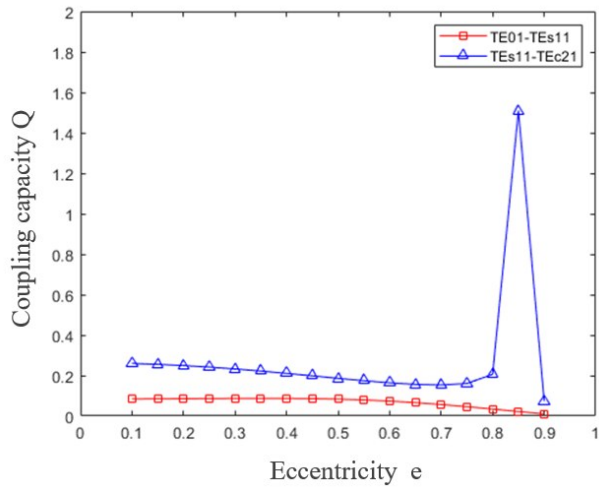
Fig. 3　The variation law of coupling ability with the eccentricity
图3　耦合能力随离心率的变化规律

culties suppressing the spurious mode TEc$_{21}$. In this paper, the coupling ability of TEs$_{11}$-TEc$_{21}$ is selected to be lower, while the coupling ability of TE$_{01}$-TEs$_{11}$ is slightly larger in the range of 0.65-0.7. Integrating the previous selection range, the selected eccentricity range is between 0.65-0.7, and finally the eccentricity e=0.7 is selected as the size of elliptic waveguide mode converter in this paper, when the short semi-axis b=12.426 mm.

After determining the elliptical cross-sectional dimensions, the phase rematching method is introduced into the elliptical waveguide longitudinal contour line[8-9].

$$
\begin{aligned}
y(z) = & e_1 \cdot a \cdot \cos\left(\frac{2\pi}{\lambda_{B1} \cdot (1+\delta_1)} \cdot z\right) - \\
& e_2 \cdot a \cdot \sin\left(\frac{2\pi}{\lambda_{B2} \cdot (1+\delta_2)} \cdot z\right) \quad , \quad (11) \\
& -e_3 \cdot a \cdot \sin\left(\frac{2\pi}{\lambda_{B3} \cdot (1+\delta_3)} \cdot z\right)
\end{aligned}
$$

where e_1, e_2, e_3 denote the perturbation amplitude, a denote the long semi-axis of the elliptical waveguide, $\delta_1, \delta_2, \delta_3$ denotes the phase re-matching factor, $\lambda_{B1}, \lambda_{B2}, \lambda_{B3}$ denote the beat frequency wavelength between TE$_{01}$ and TEs$_{11}$, TE$_{01}$ and TEs$_{12}$ and TEs$_{11}$ and TEc$_{21}$, respectively.

After determining the cross-sectional dimensions and the longitudinal contour line structure of the elliptic waveguide mode converter, the longitudinal structure needs to be optimized in order to improve the conversion efficiency of the elliptic waveguide converter. In this paper, the seven parameters of perturbation amplitude e_1, e_2, e_3 and phase rematching factor $\delta_1, \delta_2, \delta_3$ as well as the length L of the elliptic mode converter are optimized using a Particle Swarm Optimization (PSO)[4]. PSO is a method to obtain a local maximum by optimizing each

variable. In this article, we optimized seven parameters and found the maximum transmission efficiency.

The values of these seven parameters were obtained by writing a numerical calculation program in MATLAB and optimizing the parameters of the contour line structure as well as the lengths, as shown in Table 1.

Once the optimized parameters are obtained, the contour line structure of the mode variator can be derived as shown in Fig. 4.
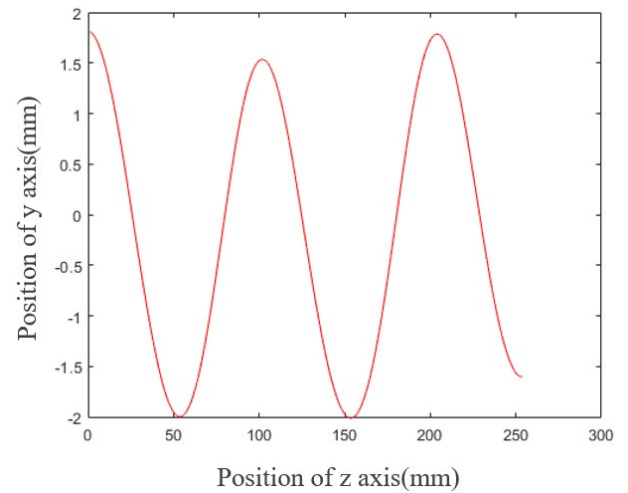

Fig. 4　Elliptical waveguide mode converter contour line
图4　椭圆波导模式转换器轮廓线

In order to make the numerically calculated efficiency more accurate, eight modes are considered in the numerical calculation procedure, respectively TE$_{01}$, TEs$_{11}$, TEs$_{12}$, TEc$_{21}$, TEs$_{21}$, TM$_{01}$, TMc$_{11}$, TMs$_{21}$. The efficiency of the TE$_{01}$-TE$_{11}$ mode converter is finally calculated to be 99.23%. The numerical simulation of the conversion process of the relative power of the mode converter is shown in Fig. 5. It can be seen from the figure that TEs$_{12}$, TEc$_{21}$ are the main heterodyne modes in this mode converter, which is consistent with the analysis above, and the relative power of these two heterodyne modes does not exceed 5% during the conversion process. In particular, TM$_{01}$, TEs$_{21}$, and TMs$_{21}$ are almost completely suppressed. It can be shown that the design of this mode converter is feasible.

Modeling and simulation are performed in CST simulation software to further verify the feasibility of the designed elliptic mode converter by analyzing the results after simulation.

The model diagram of the elliptic waveguide TE$_{01}$-TEs$_{11}$ mode changer built in CST is shown in Fig. 6. The model is next simulated and analyzed, and the efficiency of its central frequency point is obtained as 99.16%, which is consistent with the program calculation and

Table 1　The parameter table for particle swarm algorithm optimization
表1　粒子群算法优化参数表

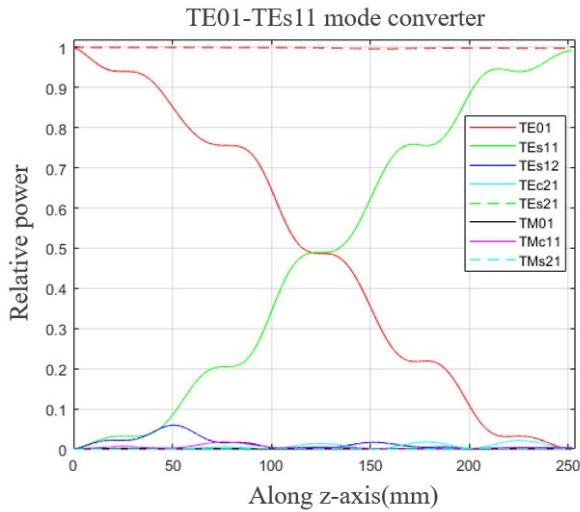| Symbol	e_1	e_2	e_3	δ_1	δ_2	δ_3	L
Value and Unit	0.1127	0.0361	0.0192	0.15	0.0038	−0.0043	253.7 mm

Fig. 5 Numerical simulation process of relative power of each mode of TE_{01}-TE_{11} mode converter
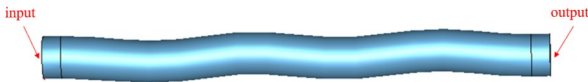
图5 TE_{01}-TE_{11}模式转换器各模式相对功率的数值模拟过程

Fig. 6 Elliptical waveguide TE_{01}-TEs_{11} mode converter model diagram

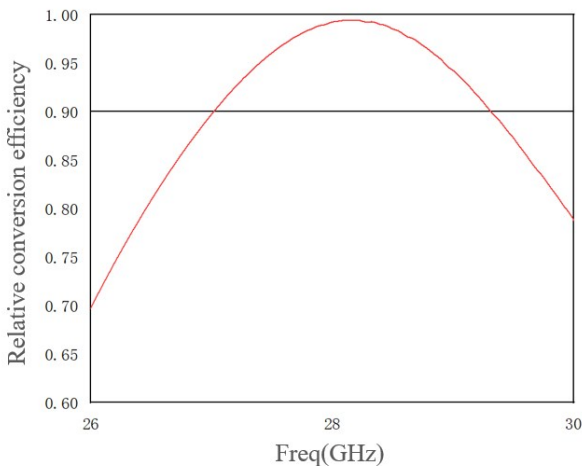图6 椭圆波导TE_{01}-TEs_{11}模式转换器模型图

Fig. 7 Elliptical waveguide TE_{01}-TEs_{11} mode converter sweep chart

图7 椭圆波导TE_{01}-TEs_{11}模式转换器扫描图

proves the correctness of the designed elliptic mode changer. Fig. 7 shows the swept frequency diagram of the mode converter obtained from the simulation, from which it can be seen that the bandwidth of the mode converter greater than 90% is 27-29.3 GHz, so the relative bandwidth is about 8.2%.

Fig. 8 shows the longitudinal profile electric field diagram of this mode converter distributed along the z-axis, from which it can be noticed that the TE_{01} mode is gradually transformed into the TEs_{11} mode.
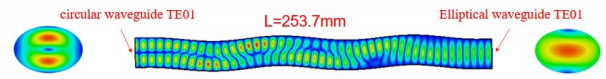
In practice, the input and output ports of the cyclo-

Fig. 8 Elliptical waveguide TE_{01}-TEs_{11} mode converter profile electric field diagram

图8 椭圆波导TE_{01}-TEs_{11}模式转换器剖面电场图

tron are usually circular waveguides, so a section of transition waveguide needs to be added to each end of the designed elliptical waveguide TE_{01}-TEs_{11}. The radius of the circular waveguide at the input and output ports of the mode converter designed in this paper is 16 mm; therefore, a section of transition from the circular waveguide TE_{01} to the elliptical TE_{01} and a section of transition from the elliptical waveguide TEs_{11} to the circular waveguide TE_{11} are required.

Since elliptical waveguides are not completely symmetrical like circular waveguides, it is difficult to design the transition profile, so the current design of the circular to the elliptical waveguide transitions usually uses direct simulation. For the circular waveguide TE_{01} to the elliptical waveguide TE_{01} transducer, the simulation is built in CST to obtain the length L1=400 mm that meets the design, and the relative conversion efficiency at the center frequency point is 99.32%. Similarly, the elliptical waveguide TEs_{11} to the circular waveguide TE_{11} transducer is modeled in CST, and a transducer length L2=105 mm is obtained in accordance with the design, with a conversion efficiency of 99.88% at the center frequency point.

The overall structure and profile electric field amplitude distribution of the TE_{01}-TE_{11} mode converter, which has an overall length of L=758.7 mm, were obtained by connecting the designed mode converter and two transition segments together in the CST, as shown in Fig. 9.

When designing devices such as mode converters, the power capacity of the device must be considered, because if the power of the mode converter is too small, it will be broken by the electric field in the vacuum, causing the firing phenomenon and thus affecting the service life of the converter. Fig. 9 shows the instantaneous electric field at the central frequency point of 28 GHz, and it can be seen that the maximum value of the total electric field amplitude is 2050 V/m. The breakdown field strength in vacuum is conservatively chosen $E_{max} = 100 kV/mm$[5]. Assuming that the power capacity of this elliptical waveguide mode converter is P_{max}, the power capacity is proportional to the square of the maximum electric field amplitude:

$$P_{max} = \left(\frac{E_{max}}{E_0} \right)^2 P_0 \qquad , \quad (12)$$

with the input power $P_o = 1W$, the maximum power capacity of the mode converter is calculated to be about 2.38 GW, which meets the power capacity requirement of the cyclotron application system.

3 Conclusion

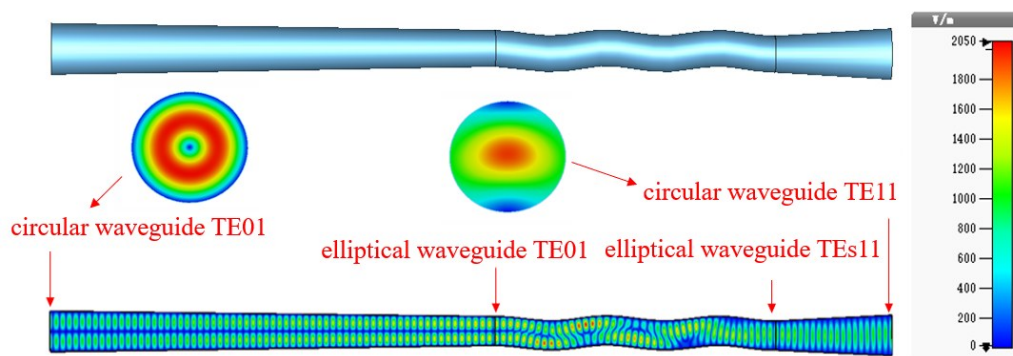In this paper, the elliptical waveguide TE_{01}-TE_{11}

Fig. 9　Elliptical waveguide TE$_{01}$-TE$_{11}$ mode converter overall structure and profile electric field distribution diagram

图9　椭圆波导TE$_{01}$-TE$_{11}$模式转换器总体结构和剖面电场分布图

mode converter is designed and studied. The design principle of elliptical waveguide TE$_{01}$-TEs$_{11}$ mode converter is analyzed. Meanwhile，the waveguide bending direction is selected according to the normalized cutoff wavelengths at different eccentricity，after that the coupling coefficients and coupling ability of TE$_{01}$-TEs$_{11}$ and TEs$_{11}$-TEc$_{21}$ are calculated. The appropriate elliptical waveguide cross-sectional dimensions were selected according to the laws of their coupling coefficients and coupling capacities. The serpentine coupling structure is adopted，and a program is written to optimize the waveguide contour line curve parameters，and the simulation is verified in CST，and the simulation results are verified to be consistent with the results calculated by the program. The designed elliptical mode converter is connected with two transitions and simulated and verified in CST. An efficient，compact，high-power，elliptical waveguide TE$_{01}$-TE$_{11}$ mode converter with center frequency point at 28 GHz is designed.

References

［1］Shanjie Zhang，Yaochun Shen. Eigenmode sequence for an elliptical waveguide with arbitrary ellipticity［J］. *IEEE transactions on microwave theory and techniques*，1995，**43**(1)：227-230.

［2］Keqiang Wang，Tianming Li，Hao Li，*et al*. A broadband TE$_{01}$－TE$_{11}$ mode converter with elliptical section for gyro-TWTs［J］. *IEEE Transactions on Microwave Theory and Techniques*，2019，**67**(9)：3586-3594.

［3］Xiaoyi Liao，Zeiwei Wu，Jianxu Wang，*et al*. Design of a TE01- mode waveguide bend based on an elliptical waveguide structure［J］. *IEEE Transactions on Microwave Theory and Techniques*，2019，**67**(3)：906-914.

［4］Robert Nshimirimana，Ajith Abraham，Gawie Nothnagel. A multi-objective particle swarm for constraint and unconstrained problems［J］. *Neural Computing and Applications*，2021(05)：1-31.

［5］J. Barker，E. Schamiloglu. High-Power Microwave Sources and Technologies. New York，NY，USA：IEEE Press，2001.

［6］Niu X，Yu X，Li S，*et al*. High-power TE01－TE11 mode converter for gyroklystron［J］. *Journal of Fusion Energy*，2013，**32**(4)：426-430.

［7］Yu X，Deng J，Cao W，et al. Method for Synthesis of TE$_{01}$-TE$_{11}$ Mode Converter for Gyrotron by the NURBS Technique［J］. Microwave Theory & Techniques IEEE Transactions on，2015，63(2)：326-330.

［8］Xu Le，Niu Xin-jian. 8mm high power TE01—TM11 mode converter in overmoded waveguide［C］. 2009 IEEE International Vacuum Electronics Conference，2009，pp. 487-488.

［9］M，THUMM. High-power millimetre-wave mode converters in overmoded circular waveguides using periodic wall perturbations［J］. International Journal of Electronics，1984，57(6)：1225-1246..

［10］G. Blanch，M. Abramowitz，I. Stegun. Handbook of Mathematical Functions［M］. Washington DC：National Bureau of Standards，chap. 20，pp. 721－750，1964.

［11］Gutiérrez-Vega J C，Rodrıguez-Dagnino R M，Meneses-Nava M A，*et al*. Mathieu functions，a visual approach［J］. *American Journal of Physics*，2003，**71**(3)：233-242.

［12］Bibby M M，Peterson A F. Accurate computation of mathieu functions［J］. *Synthesis lectures on computational electromagnetics*，2013，**8**(2)：1-133.

［13］Thumm M，Kasparek W. Passive high-power microwave components［J］. *IEEE Trans on Plasma Science*，2002，**30**(3)：755-786.

［14］Thumm M. Recent developments on high-power gyrotrons：Introduction to this special issue［J］. *Journal of Infrared*，*Millimeter*，*and Terahertz Wave*，2011，**32**(3)：241-252.